Mathematical Modelling of Engineering Problems
Vol. 10, No. 6, December, 2023, pp. 2086-2094
Journal homepage: http://iieta.org/journals/mmep

Early Detection of Diabetic Retinopathy Utilizing Advanced Fuzzy Logic Techniques

Mohammed Imran Basheer Ahmed

Department of Computer Engineering, College of Computer Science and Information Technology, Imam Abdulrahman Bin Faisal University, P.O. Box 1982, Dammam 31441, Saudi Arabia

Corresponding Author Email: mbahmed@iau.edu.sa

https://doi.org/10.18280/mmep.100619

Received: 10 July 2023
Revised: 22 August 2023
Accepted: 10 September 2023
Available online: 21 December 2023

Keywords:
Diabetic Retinopathy (DR), extended fuzzy logic (FLe), micro-aneurysms (MA), exudates, hemorrhages, ordered weighted averaging (OWA), early diagnosis, computational diagnosis

ABSTRACT

The escalating prevalence of diabetes globally, exacerbated by lifestyle changes post-pandemic—including increased screen time, sedentary behavior, and remote work—has consequently driven a surge in associated complications, notably, Diabetic Retinopathy (DR). This ocular complication presents a pressing concern due to its potential to precipitate irreversible vision loss. Consequently, the necessity for timely and accurate DR detection is paramount, especially in circumstances where conventional diagnostic approaches are either challenging or financially prohibitive. Capitalizing on the prowess of fuzzy logic in managing uncertainties, this study introduces an innovative application of Extended Fuzzy Logic for the early-stage detection of DR. Rather than focusing solely on overt symptoms, this approach discerns subtle similarities in retinal irregularities between diabetic patients and non-diabetic individuals. To quantify these similarities, the 'f-validity' value was computed based on DR risk factors and associated symptoms, which were subsequently transformed into membership function values. The aggregation of these values was facilitated by the Ordered Weighted Averaging (OWA) operator. The experimental outcomes of this approach align satisfactorily with expert anticipations, boasting an accuracy of 90%, a precision of 92.2%, and a sensitivity of 75%. These results, when juxtaposed against contemporary studies in the field, underscore the promise of this scheme in advancing early diagnostics of DR. The study thus proposes a potential solution that leverages the power of fuzzy logic to address the burgeoning challenge of DR.

1. INTRODUCTION

Diabetes, a rapidly proliferating epidemic worldwide, precipitates a myriad of associated disorders, imposing significant burdens on both patients and healthcare systems. A prominent and debilitating complication is Diabetic Retinopathy (DR), which ranks fourth among global chronic diseases [1]. DR, a disorder stemming from prolonged uncontrolled diabetes mellitus, inflicts damage on the retina's blood vessels, potentially culminating in severe vision impairment [2]. Consequently, the early diagnosis of DR is paramount, not only facilitating timely treatment but also ameliorating disease progression. A plethora of research has sought to automate DR detection, with Extended Fuzzy logic emerging as a promising tool, as initially suggested in reference [3].

Interestingly, the post-pandemic lifestyle, characterized by extended screen time, reduced physical activity, and limited social interaction, has been implicated in the increase of DR [4]. These influences are particularly pronounced in regions such as the Kingdom of Saudi Arabia, where online work predominates, and high screen time and a sedentary lifestyle are common [5].

Prompted by the need for preemptive DR management, this study aims to devise an early detection system that could potentially warn individuals about their DR risk based on their eye images captured in real-life settings. The envisioned prototype could be integrated into smartphones, offering a comprehensive health monitoring platform that includes eye imaging. Such a tool could identify potential precursors to DR, enabling users to take preventive measures before the condition advances.

The remainder of this paper is organized as follows: Section II presents the related work and describes the dataset used in this study; Section III provides a detailed account of the proposed model; Section IV reports the experimental results; and Section V concludes the paper with a brief summary of the findings and their implications.

2. LITERATURE REVIEW

The concept of fuzzy valid solution, first proposed by Lotfi Zadeh – the originator of fuzzy logic – was elaborated upon in [6]. Zadeh envisaged a world exempt of traditional tools such as rulers, compasses, and pens, wherein f-valid shapes were to be rendered using a spray pen instead. The resulting inexact, or fuzzy geometric shapes, as described in reference [7], defy categorization as either perfect geometrical entities or the complete negation thereof.

These indeterminate shapes align with Shannon's uncertainty principle. The formulation of the f-principle of geometric shapes, initiated in reference [8], defines fuzzy geometric shapes via the exponential membership function in conjunction with a mathematical function. Building on this, the concept of freehand-drawn fuzzy geometric shapes, characterized by a fuzziness level between zero and one, was explored in reference [9]. The identification and retrieval of applications of f-valid geometric shapes were subsequently addressed in reference [10].

The application of artificial neuro-fuzzy inference in the diagnosis of DR was discussed in reference [11], paralleling the recent trend of employing machine learning algorithms in the early diagnosis of other chronic diseases [12-16]. These studies have delved into a variety of machine learning algorithms, including the Support Vector Machine, K-Nearest Neighbour, Adaptive Boosting, Extreme Gradient Boosting, and Synthetic Minority Oversampling Technique, and juxtaposed their results with prior research.

The use of ensemble techniques in the study of epilepsy in both pediatric and adult populations was reported in references [17, 18]. The dynamic fuzzy rule-based system was utilized for the early diagnosis of COVID-19 patients in reference [19], taking COVID symptoms as parameters to predict the likelihood of infection. A clinical decision support system, leveraging a fuzzy rule-based system, was proposed and implemented in reference [20]. This system aimed to facilitate remote patient care from urban doctors through communication channels, utilizing data mining techniques such as the Apriori algorithm, inductive learning, and the British National Formulary (BNF) database.

The concept of fuzzy prediction using new soft computing was introduced to supersede previous forecasting methodologies [21]. This approach employed event discretization of time series, frequency partitioning, and optimization. Predicting the average length of a patient's stay based on past data was discussed in reference [22], with a view to forecasting the allocation of patient facilities in advance. Transfer learning, a specialty of deep learning, was proposed as a tool for predicting various diseases in the healthcare sector [23-27].

The application of Deep Learning in the detection of DR from early to late stages was reported in reference [28]. The real-time analysis of DR achieved an accuracy ranging from 90% to 96%, with external validations yielding results of up to 97%. The authors in reference [29] reviewed various methods of segmentation, classification, and constraint calculation for DR. They conducted a statistical analysis of DR detection and classification with a comprehensive literature review spanning 2000 to 2021, examining over 800 documents. They recommended focusing on balanced and multimodal datasets, semi-supervised, self-supervised, and deep neural networks.

The authors in reference [30] underscored the need for intelligent methods for DR diagnosis, to supplant the time-consuming and potentially error-prone manual screening of DR fundus images. They suggested that convolutional neural networks could be used for classification and detection of DR in fundus retinal image datasets. The potential of Artificial Intelligence in ensuring accurate diagnoses of DR was explored [31]. The authors asserted that pattern recognition, which facilitates complex relationships between input and output image comparisons of DR, could simplify the detection of retinal disorders, including DR, for ophthalmologists.

3. DATASET

To evaluate the early DR detection method, the publicly available DIARETDB1 database is used. The database consists of 89 eye fundus color images of which 84 comprises the mild signs of Diabetic Retinopathy (Micro-aneurysms), and 5 are considered normal which do not contain any DR related signs. Diabetic Retinopathy Images were taken using 50-degree view position with digital fundus camera with different imaging situations [32]. For the implementation, MATLAB software version R2015b has been used.

4. DESCRIPTION OF THE PROPOSED TECHNIQUES

The process of finding the damage percentage of the retina which is caused by Diabetic Retinopathy requires some of the fundamental constraints that are described in [3]. First the medical knowledge which is considered as Diabetic Retinopathy risk factors, will be taken from the diabetic patient. This information includes duration of diabetes, glycemic level, hypertension level, cholesterol level and hemoglobin blood level. Then the difference will be computed for each risk factor which will be done by subtracting them from the normal values. Then the number of infected regions by each Diabetic Retinopathy sign will be counted. That will be done by taking the retinal fundus image of the patient eye to detect the three signs associated with Diabetic Retinopathy which are micro-aneurysms, hemorrhages and exudates. To ensure accurate detection of the symptoms the retinal landmarks must be extracted first as they have similarities with the DR signs. The retina has three main landmarks which are optic disc, blood vessels and fovea.

4.1 Optic disk extraction

The optic disk must be removed because it exhibits the same bright color as the exudates. The method was implemented based on the proposed methodology described in reference [33]. The method starts by taking the intensity channel of the input image and applying a median filter to reduce the noise. Then the difference of every tiny region was improved by applying adaptive histogram equalization (CLAHE).

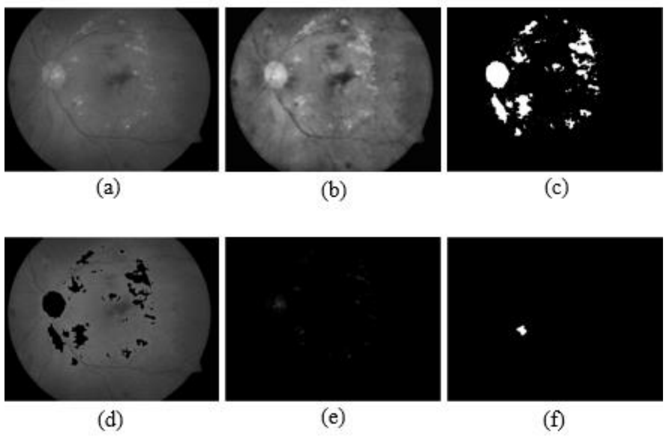

Figure 1. The steps for the optic disk localization algorithm: (a) The intensity channel; (b) The result of applying a closing operator; (c) The threshold image;(d) The result of complementing and overlaying IMG2; (e) The result of the subtraction; (f) The final image

The optic disc has high intensity value as well as the blood vessels, thus the blood vessels are removed by applying a closing operator on the enhanced image resulting in IMG1. Then, thresholding IMG1 to get IMG2, the value of the threshold was determined by selecting the brightest 5% of the pixels. IMG2 is then complemented and overlaid on the intensity channel to get IMG4 which is used as a marker in the next step which is the morphological reconstruction with the intensity channel as a marker resulting in IMG5. IMG5 is then subtracted from the intensity image resulting in IMG6 and threshold using the Otsu algorithm to get IMG7. Since the optic disc is usually the largest area in the resulted image, the largest component was selected as the optic disc or part of it and then the centroid and major axis length was calculated to be used in extracting the optic disc completely. Figure 1 illustrates the result of each operation.

4.2 Blood vessels extraction

Another necessary landmark to be extracted is the blood vessels as they exhibit the same color as Micro-aneurysms and Hemorrhages. The algorithm for the blood vessels was implemented based on the proposed methodology described in [34]; the algorithm starts with converting the image into grayscale using Craig's formula to get IMG1. At first, an opening operator with a disk element of radius three was applied to IMG1 to remove minor noise and get IMG2. A closing operation is then applied on IMG2 with a disk element of radius eight to eliminate the blood vessels and get IMG3. A top hat transformation is then applied on IMG3 to get the high contrast blood vessels image. Finally, to reduce the noise, only the largest blood vessels are in the final image. Figure 2 illustrates the result of each operation.

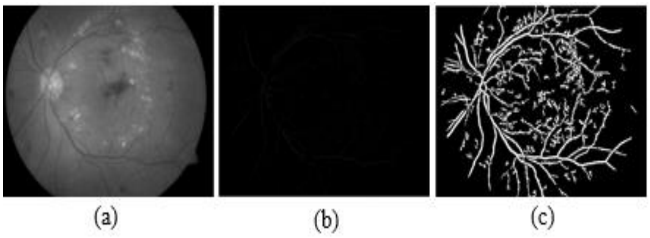

Figure 2. The steps for the blood vessels extraction algorithm: (a) The RGB Luminance value with reduced noise; (b) The result of Top-Hat transformation; (c) The extracted blood vessels

4.3 Fovea extraction

The fovea, which is the last landmark, is removed because it also exhibits the same color as Micro-aneurysms and Hemorrhages. The method used to extract the fovea is the same as the method used for hemorrhages which will be discussed later in this paper except that the threshold value is obtained by taking the mean value of the green channel instead of the red channel in the hemorrhages. At the end the largest object is selected to be the fovea.

4.4 Micro-aneurysms detection

The first DR sign that needs to be detected is the Micro-aneurysms (MA). The detection of Micro-aneurysms was implemented based on the proposed methodology described in reference [35].

The retina image must be set to size 752×500 to make the diameter of the micro-aneurysms about 10 pixels.

Then, the green channel (IMG1) of the RGB image is taken since the red lesions such as Micro-aneurysms and blood vessels have the highest contrast with the surroundings of retina in this channel. A median filtering operation of 35×35 is then harnessed before applying the contrast limited adaptive histogram equalization (IMG2). After that, shade correction is applied using a low pass filter (IMG3) to correct the background variation.

The blood vessels must be eliminated from the original image to get IMG4. The extended-minimum transformation is used on the shaded corrected image IMG3 to get IMG5 with threshold value of 12. The result image IMG5 is a binary image with the white pixels representing the regional minimum in the original image. Then, the previously detected blood vessels IMG4 is deducted from the resulting image IMG5. The final step is detecting the micro-aneurysms on the image, which are the regions that have the size of 10 pixels. Figure 3 illustrates the result of each operation.

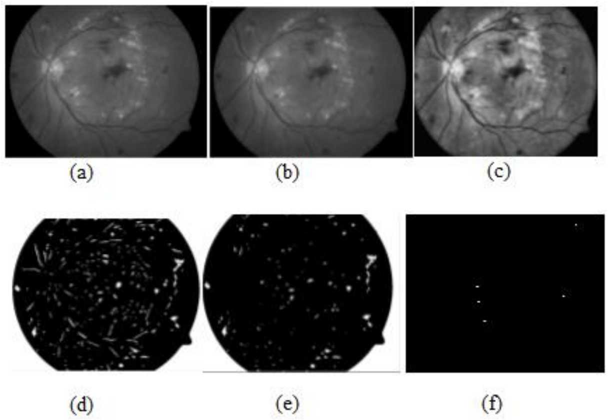

Figure 3. Shows the steps for the Micro- aneurysm detection algorithm: (a) the filtered green channel; (b) noise removal; (c) Shade corrected image; (d) Extended-Minima transform; (e) Image after blood vessels removal; (f) the detected Micro-aneurysm

4.5 Hemorrhages detection

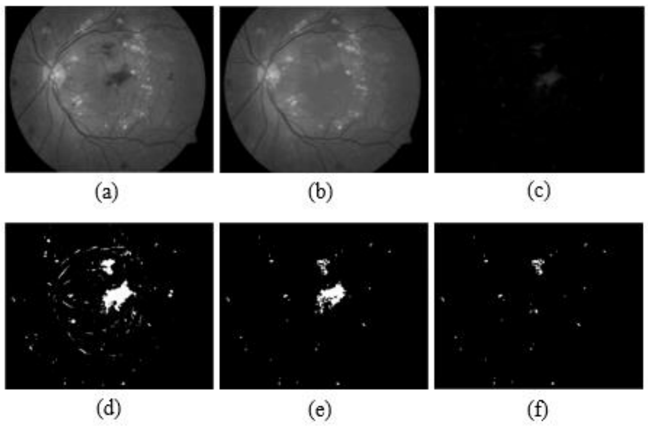

Figure 4. The steps for hemorrhages detection algorithm: (a) Green channel of input image; (b) Filled green image; (c) The result of subtracting the green channel from the filled image; (d) The result of thresholding IMG3; (e) Image without the blood vessels and the fovea; (f) Final image

For detecting the second sign Hemorrhages which appears like micro-aneurysms but bigger in size, the method discussed [36] was implemented. The method begins with extracting the green channels of the input fundus image (IMG1); then morphological filling is carried-out on the extracted green channel to recognize the red lesions which are micro-aneurysms and Hemorrhages (IMG2). Then the green channel image is deducted from the unfilled green channel to remove all the dark regions appearing in both the filled green channel and the unfilled one (IMG3).

IMG3 is then applied to the threshold according to the intensity by using the average pixels value in the red channel of the input image as a threshold value (IMG4). Then, the blood vessels extracted image and the fovea image are subtracted from IMG4 to remove all the regions belonging to them (IMG5).

Finally, all the regions which are bigger than 40 pixels have been considered as Hemorrhages. Figure 4 illustrates the result of each operation [37, 38].

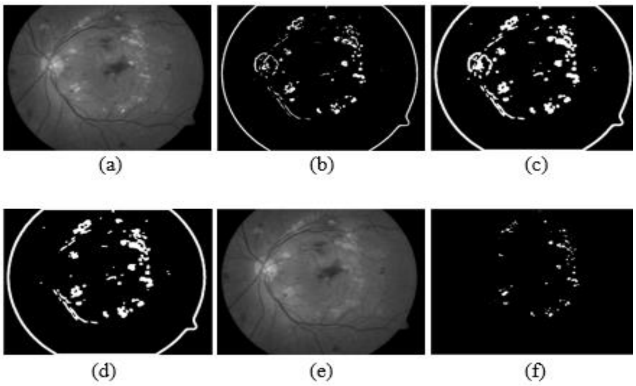

Figure 5. The steps for the exudates detection algorithm: (a) the filtered green channel; (b) The result of thresholding the filtered image; (c) The reconstructed image using IMG4, IMG5; (d) Image without optic disc; (e) The reconstructed image using IMG9, Green Channel; (f) The extracted exudates

4.6 Exudates detection

The last DR sign that needs to be detected is the exudates. This method was implemented based on the proposed methodology described [39]. First, a Gaussian filter is used to the input image to reduce the noise. Then, the green channel is taken since the exudates and blood vessels regions have high contrast; blood vessels are excluded by using a morphological closing to get IMG1. The exudates candidate regions are then achieved by calculating the local variation of each pixel in IMG1 and thresholding the resulted image (IMG2) to get IMG3. IMG3 contains the borders of bright large object and small bright objects and to get the entire candidate regions, IMG3 is dilated to get IMG4. Then IMG4 is eroded with an element half size the previous one to get IMG5. Both IMG4 and IMG5 are then used to perform morphological reconstruction to get IMG6. Since optic disk and exudates have bright colors, the optic disk is eliminated by subtracting a dilated version of it from IMG6 to get IMG7. After that, the regions in IMG7 are set to zero in the green channel to get IMG8. Then a reconstruction operator is applied using the green channel as a mask and IMG8 as maker to get IMG9. The binary image is then accomplished by employing a threshold to the difference between the green channel image and IMG9. Finally, the remaining blood vessels are eliminated by subtracting the blood vessels from the binary image. The following Figure 5 illustrates the result of each operation.

After finding the difference in Diabetic Retinopathy risk factors and the signs, the f-validity computation begins by using the exponential membership function. The f-theorem will be used to find the f-validity which is represented as following:

$$\mu(f - theorem) = \mu 1 * \mu 2 * \mu 3 \ldots .* \mu n \tag{1}$$

$$\mu = e^{-|d|} \tag{2}$$

Then, OWA is used to aggregate the membership function values which gives the final f-validity value.

4.7 Ordered weighted averaging (OWA) operator

An OWA operator [40] of element ‘n’ is a mapping Ordered Weighted Averaging such that: Rn → R that has an associated set of weights: $w=(w_1, w_2,..,w_n)$T to the vector a_i(i=1, 2, 3, ..., n) such that:

$$\sum_{i=0}^{n} w_i = 1 \; and \; w_i \in [0,1] \tag{3}$$

So, $F(a_1, a_2, \ldots, a_n) = \sum_{i=1}^{n} w_i a_{\sigma(i)}$, where, $\sigma = 1, 2, 3 \ldots . n$.

$a_{\sigma(i)}$ is the biggest value in the set (a_1, a_2, ..., a_n) such that

$$a_{\sigma(i)} \geq a_{\sigma(i-1)}$$

The final f-validity will be the combination of the f-theorem and OWA which can be represented as following:

$$\text{f-validity}=\sum_{i=0}^{n} w_i \mu \tag{4}$$

5. RESULTS OF EXPERIMENT AND DISCUSSION

As was discussed in section 2, DIARETDB1 database was used to evaluate the model. Around 30 images were taken from the dataset and their medical information was specified by an expert along with his final expected results which were compared against the system's results. In this section a detailed example will be illustrated for different cases mild, moderate, sever and normal.

Table 1 summarizes the result of different cases.

Mild

Figure 6 shows a retinal fundus image which belongs to the mild Diabetic Retinopathy level. The expert specified the medical information for this case as 15 years for diabetes duration, 7.3 for A1C test, 125/74 for blood pressure, 112 for cholesterol level and 16 for hemoglobin blood level. The number of Micro-aneurysms detected is 3, number of Hemorrhages detected is 1 and the number of exudates is 5.

Using the medical information the difference between the patient's information, the normal values and the number of infected regions will result in the input differences which are [15, 1.7, 0, 0, 0, 0, 3, 1, 5], the membership function values are [3.05×10^{-6}, 0.1827, 1, 1, 1, 1, 0.0498, 0.3679, 0.0067] and for these nine parameters the weight vector is [0.1587, 0.1587, 0.1587, 0.1587, 0.1587, 0.1587, 0.0476, 0, 0]. Using the OWA operator, the f-validity is computed result is 0.72468.

Table 1. Samples of the result

Image	Duration	A1C	Blood Pressure	Cholesterol Level	HB Blood Level	Expected Result	F-Validity
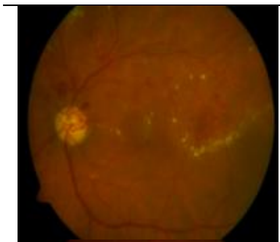	21	7.8	148/86	175	15.8	Moderate	0.64934
	25	8.6	150/86	208	17	High	0.32539
	15	7	125/80	120	16	Low	0.68434
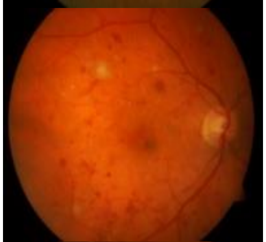	21	8.1	136/79	170	15.5	Moderate	0.64795
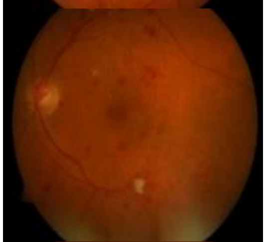	26	8.5	148/86	185	16.5	High	0.32627
	0	5.1	120/80	230	15.2	Normal	1
	0	4.7	125/85	253	12.5	Normal	0.9525
	17	8	138/79	125	15.8	Moderate	0.65235

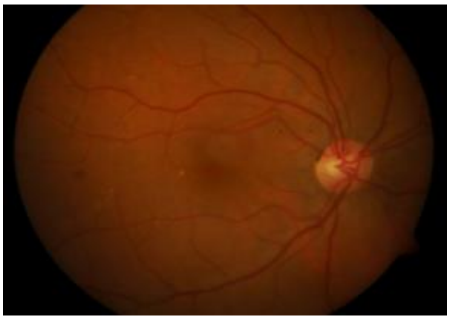

Figure 6. Fundus image with mild DR

f-validity=[1 1 1 1 0.3679 0.1827 0.0498 0.0067 3.05×10^{-6}] * [0.1587 0.1587 0.1587 0.1587 0.1587 0.1587 0.0476 0 0]
=[(1* 0.1587)+(1 * 0.1587)+(1 * 0.1587)+(1 * 0.1587)+(0.3679 * 0.1587)+(0.1827* 0.1587)+(0.0498 * 0.0476)+(0.0067 * 0)+(3.05×10-6* 0)]
=0.72468

Moderate

Figure 7 shows a retinal fundus image which belongs to the moderate Diabetic Retinopathy level. The expert specified the medical information for this case as 23 years for diabetes duration, 7.9 for A1C test, 123/75 for blood pressure, 130 for cholesterol level and 16 for hemoglobin blood level. The number of Micro-aneurysms detected is 17, the number of Hemorrhages detected is 47 and the number of exudates is 18.

Using the medical information the difference between the patient's information, the normal values and the number of infected regions will result in the input differences which are [23, 2.3, 0, 0, 0, 0, 17, 47, 18], the membership function values are [1.0262×10^{-10}, 0.1003, 1, 1, 1, 1, 4.1399×10^{-8}, 3.8740×10^{-21}, 1.523×10^{-8}] and for these nine parameters the weight vector is [0.1587, 0.1587, 0.1587, 0.1587, 0.1587, 0.1587, 0.0476, 0, 0].

Figure 7. Fundus image with moderate DR

Using the OWA operator, the f-validity is computed as:

f-validity=[1 1 1 1 0.1003 4.1399×10^{-8} 1.523×10^{-8} 1.0262 ×10^{-10} 3.8740×10^{-21}] * [0.1587 0.1587 0.1587 0.1587 0.1587 0.1587 0.0476 0 0]
=[(1 * 0.1587)+(1 * 0.1587)+(1 * 0.1587)+(1 * 0.1587)+(0.1003 * 0.1587)+(4.1399×10^{-8} * 0.1587)+(1.523×10^{-8} * 0.0476)+(1.0262×10^{-10} * 0)+(3.8740 ×10^{-21} * 0)]
=0.65083

Severe

Figure 8 shows a retinal fundus image which belongs to the sever DR level. The expert specified the medical information for this case as 22 years for diabetes duration, 8.1 for A1C test, 148/74 for blood pressure, 180 for cholesterol level and 16.5 for hemoglobin blood level. The number of Micro-aneurysms detected is 27, number of Hemorrhages detected is 38 and the number of exudates is 87.

Figure 8. Fundus image with severe DR

Figure 9. Fundus image with normal DR

Using the medical information the difference between the patient's information, the normal values and the number of infected regions will result in the input differences which are [22, 2.5, 8, 21, 0, 0, 27, 38, 86], the membership function values are [2.7895×10^{-10}, 0.0821, 3.3546×10^{-4}, 7.5826×10^{-10}, 1, 1, 1.8795×10^{-12}, 3.1391×10^{-17}, 4.4738×10^{-38}] and for these nine parameters the weight vector is [0.1587, 0.1587, 0.1587, 0.1587, 0.1587, 0.1587, 0.0476, 0, 0]. Using the OWA operator, the f-validity is computed as

f-validity=[1 1 0.0821 3.3546×10^{-4} 7.5826×10^{-10} 2.7895×10^{-10} 1.8795x10^{-12} 3.1391×10^{-17} 4.4738×10^{-38}] * [0.1587 0.1587 0.1587 0.1587 0.1587 0.1587 0.0476 0 0]
=[(1 * 0.1587)+(1 * 0.1587)+(0.0821* 0.1587)+(3.3546×10^{-4}* 0.1587)+(7.5826×10^{-10} * 0.1587)+(2.7895×10^{-10} * 0.1587)+(1.8795×10^{-12} * 0.0476)+(3.1391×10^{-17} * 0)+(4.4738×10^{-38} * 0)] =0.33054

Normal

Figure 9 shows a retinal fundus image which belongs to the Normal case. The expert specified the medical information for this case as 0 years for diabetes duration, 4.5 for A1C test, 123/75 for blood pressure, 220 for cholesterol level and 15.8 for hemoglobin blood level. The number of Diabetic Retinopathy signs is 0 meaning Diabetic Retinopathy signs are not presented.

Using the medical information, the difference between the patient's information, the normal values and the number of infected regions will result in the input differences which are [0, 0, 0, 0, 0, 0, 0, 0, 0], the membership function values are [1, 1, 1, 1, 1, 1, 1, 1, 1] and for these nine parameters the weight vector is [0.1587, 0.1587, 0.1587, 0.1587, 0.1587, 0.1587, 0.0476, 0, 0]. Using the OWA operator, the f-validity result is 1.

f-validity=[1 1 1 1 1 1 1 1 1] * [0.1587 0.1587 0.1587 0.1587 0.1587 0.1587 0.0476 0 0]
=[(1* 0.1587)+(1 * 0.1587)+(1 * 0.1587)+(1 * 0.1587)+(1 * 0.1587)+(1 * 0.1587)+(1 * 0.0476)+(1 * 0)+(1 * 0)]=1

5.1 Model evaluation

The performance of system was evaluated by matching the expert's expectation with the f-validity range then overall accuracy, sensitivity and precision were computed, which defined as [41-50]:

$$\text{Accuracy}=\frac{TP+TN}{TP+TN+FP+FN} \tag{5}$$

$$\text{Sensitivity}=\frac{TP}{TP+FN} \tag{6}$$

$$\text{Precision}=\frac{TP}{TP+FP} \tag{7}$$

Table 2 illustrates the confusion matrix.

Table 2. Confusion matrix

	Not Damaged	Low	Moderate	High
Not damaged	10	0	0	0
Low	0	6	1	1
Moderate	0	0	8	0
High	0	0	0	4

The overall model accuracy is 90%. The sensitivity and the precision for each class are illustrated in Table 3:

Table 3. Sensitivity and precision

	Not Damaged	Mild	Moderate	High
Sensitivity	100	75	100	100
Precision	100	100	88.8	80

6. CONCLUSION

In this paper, we have illustrated the result of using Extended Fuzzy logic to diagnose Diabetic Retinopathy at an early stage where traditional facility is not available or not possible to have a provable methodology to assess the disorders of diabetic patients' eye. Basically, we have estimated the f-validity value by taking into consideration the Diabetic Retinopathy risk factors and its signs. Furthermore, the Ordered Weighted Averaging operators are devoted to aggregate the membership values of Diabetic Retinopathy features. Certainly, this discussion is not restricted to DR, instead, it leads to diagnosing more diseases by assessing the f-validity value. Moreover, the application of f-validity can be applied to various fields such as manufacturing, structural and architectural design, forensics, pattern recognition and Image retrieval. In future, it is intended to use type II fuzzy as well as deep learning and machine learning to further improve the results [51-55].

REFERENCES

[1] Prentašić, P., Lončarić, S., Vatavuk, Z., Benčić, G., Subašić, M., Petković, T., Dujmović, L., Malenica-Ravlić, M., Budimlija, N., Tadić, R. (2013). Diabetic Retinopathy image database (DRiDB): A new database for Diabetic Retinopathy screening programs research. In 2013 8th International Symposium on Image and Signal Processing and Analysis (ISPA), Trieste, Italy, pp. 711-716. https://doi.org/10.1109/ISPA.2013.6703830

[2] Habashy, S.M. (2013). Identification of Diabetic Retinopathy stages using fuzzy C-means classifier. International Journal of Computer Applications, 77(9): 7-13.

[3] Imran, M., Al-Abdullatif, A.M., Al-Awwad, B.S., Alwalmani, M.M., Al-Suhaibani, S.A., Al-Sayah, S.A. (2016). Towards early detection of Diabetic Retinopathy using extended fuzzy logic. International Journal of Pharma Medicine and Biological Sciences, 5(2): 99-98. https://doi.org/10.18178/ijpmbs.5.2.110-114

[4] Naqvi, R.A., Mushtaq, M.F., Mian, N.A., Khan, M.A., Yousaf, M.A., Umair, M., Majeed, R. (2021). Coronavirus: A "mild" virus turned deadly infection. Computers, Materials and Continua, 67(2): 2631-2646. http://dx.doi.org/10.32604/cmc.2021.012167

[5] Ahmed, M.S., Rahman, A., AlGhamdi, F., AlDakheel, S., Hakami, H., AlJumah, A., AlIbrahim, Z., Youldash, M., Alam Khan, M.A., Basheer Ahmed, M.I. (2023). Joint diagnosis of pneumonia, COVID-19, and tuberculosis from chest X-ray images: A deep learning approach. Diagnostics, 13(15): 2562. https://doi.org/10.3390/diagnostics13152562

[6] Garg, B., Sufyan Beg, M.M., Ansari, A.Q., Imran, B.M. (2011). Soft computing model to predict average length of stay of patient. In: Dua, S., Sahni, S., Goyal, D.P. (eds) Information Intelligence, Systems, Technology and Management. ICISTM 2011. Communications in Computer and Information Science, vol 141. Springer, Berlin, Heidelberg. https://doi.org/10.1007/978-3-642-19423-8_24

[7] Imran, B.M., Beg, M.S. (2011). Elements of sketching with words. International Journal of Granular Computing, Rough Sets and Intelligent Systems, 2(2): 166-178. https://doi.org/10.1504/IJGCRSIS.2011.043371

[8] Imran, B.M., Beg, M.S. (2011). Towards Computational forensics with f-geometry. In World Conference on Soft Computing.

[9] Imran, B.M., Beg, M.M.S. (2012). Fuzzy identification of geometric shapes. In: Meghanathan, N., Chaki, N., Nagamalai, D.(eds) Advances in Computer Science and Information Technology. Computer Science and Information Technology. CCSIT 2012. Lecture Notes of the Institute for Computer Sciences, Social Informatics and Telecommunications Engineering, vol 86. Springer, Berlin, Heidelberg. https://doi.org/10.1007/978-3-642-27317-9_28

[10] Ahmed, M.I.B., Alotaibi, S., Dash, S., Nabil, M., AlTurki, A.O. (2022). A review on machine learning approaches in identification of pediatric epilepsy. SN Computer Science, 3(6): 437. https://doi.org/10.1007/s42979-022-01358-9

[11] Imran, M., Alsuhaibani, S.A. (2019). A neuro-fuzzy inference model for Diabetic Retinopathy classification. In Intelligent Data Analysis for Biomedical Applications, pp. 147-172. Academic Press. https://doi.org/10.1016/B978-0-12-815553-0.00007-0

[12] Olatunji, S.O., Alansari, A., Alkhorasani, H., Alsubaii, M., Sakloua, R., Alzahrani, R., Farooqui, M., Ahmed, M.I.B., Alhiyafi, J. (2022). Preemptive diagnosis of

Alzheimer's disease in the eastern province of Saudi Arabia using computational intelligence techniques. Computational Intelligence and Neuroscience, 2022: 5476714. https://doi.org/10.1155/2022/5476714
[13] Alassaf, R.A., Alsulaim, K.A., Alroomi, N.Y., Alsharif, N.S., Aljubeir, M.F., Olatunji, S.O., Alahmadi, A.Y., Imran, M., Alzahrani, R.A., Alturayeif, N.S. (2018). Preemptive diagnosis of diabetes mellitus using machine learning. In 2018 21st Saudi Computer Society National Computer Conference (NCC), Riyadh, Saudi Arabia, pp. 1-5. https://doi.org/10.1109/NCG.2018.8593201
[14] Alassaf, R.A., Alsulaim, K.A., Alroomi, N.Y., Alsharif, N.S., Aljubeir, M.F., Olatunji, S.O., Alahmadi, A.Y., Imran, M., Alzahrani, R.A., Alturayeif, N.S. (2018). Preemptive diagnosis of chronic kidney disease using machine learning techniques. In 2018 International Conference on Innovations in Information Technology (IIT), Al Ain, United Arab Emirates, pp. 99-104. https://doi.org/10.1109/INNOVATIONS.2018.8606040
[15] Olatunji, S.O., Alotaibi, S., Almutairi, E., Alrabae, Z., Almajid, Y., Altabee, R., Altassan, M., Ahmed, M.I.B., Farooqui, M., Alhiyafi, J. (2021). Early diagnosis of thyroid cancer diseases using computational intelligence techniques: A case study of a Saudi Arabian dataset. Computers in Biology and Medicine, 131: 104267. https://doi.org/10.1016/j.compbiomed.2021.104267
[16] Olatunji, S.O., Alansari, A., Alkhorasani, H., Alsubaii, M., Sakloua, R., Alzahrani, R., Alsaleem, Y., Almutairi, M., Alhamad, N., Alyami, A., Alassaf, R., Farooqui, M., Ahmed, M.I.B. (2022). A novel ensemble-based technique for the preemptive diagnosis of rheumatoid arthritis disease in the eastern province of Saudi Arabia using clinical data. Computational and Mathematical Methods in Medicine, 2022: 2339546. https://doi.org/10.1155/2022/2339546
[17] Olatunji, S.O., Alzahrani, A., Alsubaie, A., Aldahlan, O., Alnafea, I., Alamri, A., Ahmed, M.I.B., Khan, M.A.A., Almuhaidib, A., Alhiyafi, J. (2023). Machine learning based preemptive diagnosis of Parkinson's Disease using saudi clinical data: A preliminary case study on saudi arabia dataset. In Fourth International Conference on Intelligent Data Science, Kuwai, Kuwait, pp. 1-6. http://doi.org/10.1109/IDSTA58916.2023.10317845
[18] Alotaibi, S.M., Basheer, M.I., Khan, M.A. (2021). Ensemble machine learning based identification of pediatric epilepsy. Computers, Materials & Continua, 68(1): 149-165. http://doi.org/10.32604/cmc.2021.015976
[19] Ahmed, M.I.B. (2019). Virtual clinic: A CDSS assisted telemedicine framework. In Telemedicine Technologies, pp. 227-23. Academic Press. https://doi.org/10.1016/B978-0-12-816948-3.00015-5
[20] Jan, F., Rahman, A., Busaleh, R. et al. (2023). Assessing acetabular index angle in infants: A deep learning-based novel approach. Journal of Imaging, 9(11): 242. https://doi.org/10.3390/jimaging9110242
[21] Garg, B., Sufyan Beg, M.M., Ansari, A.Q., Imran, B.M. (2011). Fuzzy time series prediction model. In: Dua, S., Sahni, S., Goyal, D.P. (eds) Information Intelligence, Systems, Technology and Management. ICISTM 2011. Communications in Computer and Information Science, vol 141. Springer, Berlin, Heidelberg. https://doi.org/10.1007/978-3-642-19423-8_14
[22] Alqarni, A., Rahman, A. (2023). Arabic Tweets-based Sentiment Analysis to investigate the impact of COVID-19 in KSA: A deep learning approach. Big Data and Cognitive Computing, 7(1): 16. https://doi.org/10.3390/bdcc7010016
[23] Ibrahim, N.M., Gabr, D.G., Rahman, A., Musleh, D., AlKhulaifi, D., AlKharraa, M. (2023). Transfer learning approach to seed taxonomy: A wild plant case study. Big Data and Cognitive Computing, 7(3): 128. https://doi.org/10.3390/bdcc7030128
[24] Abbas, T., Fatima, A., Shahzad, T., Alissa, K., Ghazal, T.M., Al-Sakhnini, M.M., Abbas, S., Khan, M.A., Ahmed, A. (2023). Secure IoMT for disease prediction empowered with transfer learning in healthcare 5.0, the concept and case study. IEEE Access, 11: 39418-39430. https://doi.org/10.1109/ACCESS.2023.3266156
[25] Asif, R.N., Abbas, S., Khan, M.A., Sultan, K., Mahmud, M., Mosavi, A. (2022). Development and validation of embedded device for electrocardiogram arrhythmia empowered with transfer learning. Computational Intelligence and Neuroscience, 2022: 5054641. https://doi.org/10.1155/2022/5054641
[26] Nasir, M.U., Zubair, M., Ghazal, T.M., Khan, M.F., Ahmad, M., Rahman, A.U., Hamadi, H.A., Khan, M.A., Mansoor, W. (2022). Kidney cancer prediction empowered with blockchain security using transfer learning. Sensors, 22(19): 7483. https://doi.org/10.3390/s22197483
[27] Nasir, M.U., Khan, S., Mehmood, S., Khan, M.A., Rahman, A.U., Hwang, S.O. (2022). IoMT-based osteosarcoma cancer detection in histopathology images using transfer learning empowered with blockchain, fog computing, and edge computing. Sensors, 22(14): 5444. https://doi.org/10.3390/s22145444
[28] Dai, L., Wu, L., Li, H., et al. (2021). A deep learning system for detecting Diabetic Retinopathy across the disease spectrum. Nature Communications, 12(1): 3242. https://doi.org/10.1038/s41467-021-23458-5
[29] Subramanian, S., Mishra, S., Patil, S., Shaw, K., Aghajari, E. (2022). Machine learning styles for Diabetic Retinopathy detection: A review and bibliometric analysis. Big Data and Cognitive Computing, 6(4): 154. https://doi.org/10.3390/bdcc6040154
[30] Alyoubi, W.L., Shalash, W.M., Abulkhair, M.F. (2020). Diabetic Retinopathy detection through deep learning techniques: A review. Informatics in Medicine Unlocked, 20: 100377. https://doi.org/10.1016/j.imu.2020.100377
[31] Padhy, S.K., Takkar, B., Chawla, R., Kumar, A. (2019). Artificial intelligence in Diabetic Retinopathy: A natural step to the future. Indian Journal of Ophthalmology, 67(7): 1004. https://doi.org/10.4103/ijo.IJO_1989_18
[32] Kauppi, T., Kalesnykiene, V., Kamarainen, J.K., Lensu, L., Sorri, I., Raninen, A., Voutilainen, R., Uusitalo, H., Kälviäinen, H., Pietilä, J. (2007). The diaretdb1 Diabetic Retinopathy database and evaluation protocol. In BMVC, 1(1): 1-18.
[33] Sopharak, A., Uyyanonvara, B., Barman, S., Williamson, T.H. (2008). Automatic detection of Diabetic Retinopathy exudates from non-dilated retinal images using mathematical morphology methods. Computerized Medical Imaging and Graphics, 32(8): 720-727. https://doi.org/10.1016/j.compmedimag.2008.08.009
[34] Samanta, S., Saha, S.K., Chanda, B. (2011). A simple and fast algorithm to detect the fovea region in fundus retinal image. In 2011 Second International Conference

on Emerging Applications of Information Technology, Kolkata, India, pp. 206-209. https://doi.org/10.1109/EAIT.2011.22
[35] Sopharak, A., Uyyanonvara, B., Barman, S. (2012). Fine microaneurysm detection from non-dilated Diabetic Retinopathy retinal images using a hybrid approach. In Proc. of the World Congress on Engineering, London, U.K.
[36] Ravishankar, S., Jain, A., Mittal, A. (2009). Automated feature extraction for early detection of Diabetic Retinopathy in fundus images. In 2009 IEEE Conference on Computer Vision and Pattern Recognition, Miami, FL, USA, pp. 210-217. https://doi.org/10.1109/CVPR.2009.5206763
[37] Qamar, R.A., Sarfraz, M., Rahman, A., Ghauri, S.A. (2023). Multi-criterion multi-UAV task allocation under dynamic conditions. Journal of King Saud University-Computer and Information Sciences, 35(9): 101734. https://doi.org/10.1016/j.jksuci.2023.101734
[38] Yager, R.R. (1988). On ordered weighted averaging aggregation operators in multicriteria decision making. IEEE Transactions on Systems, Man, and Cybernetics 18(1): 183-190. https://doi.org/10.1109/21.87068
[39] Walter, T., Klein, J.C., Massin, P., Erginay, A. (2002). A contribution of image processing to the diagnosis of Diabetic Retinopathy-detection of exudates in color fundus images of the human retina. IEEE Transactions on Medical Imaging, 21(10): 1236-1243. https://doi.org/10.1109/TMI.2002.806290
[40] Yager, R.R. (1988). On ordered weighted averaging aggregation operators in multicriteria decision making. IEEE Transactions on Systems, Man, and Cybernetics 18(1): 183-190. https://doi.org/10.1109/21.87068
[41] Ahmed, M.I.B., Alotaibi, R.B., Al-Qahtani, R.A., Al-Qahtani, R.S., Al-Hetela, S.S., Al-Matar, K.A., Al-Saqer, N.K., Rahman, A., Saraireh, L., Youldash, M., Krishnasamy, G. (2023). Deep learning approach to recyclable products classification: Towards sustainable waste management. Sustainability, 15(14): 11138. https://doi.org/10.3390/su151411138
[42] Olatunji, S.O., Alsheikh, N., Alnajrani, L., Alanazy, A., Almusairii, M., Alshammasi, S., Alansari, A., Zaghdoud, R., Alahmadi, A., Ahmed, M.I.B., Ahmed, M.S., Alhiyafi, J. (2023). Comprehensible machine-learning-based models for the pre-emptive diagnosis of multiple sclerosis using clinical data: A retrospective study in the Eastern Province of Saudi Arabia. International Journal of Environmental Research and Public Health, 20(5): 4261. https://doi.org/10.3390/ijerph20054261
[43] Sajid, N.A., Rahman, A., Ahmad, M., Musleh, D., Basheer Ahmed, M.I., Alassaf, R., Chabani, S., Ahmed, M.S., Salam, A.A., AlKhulaifi, D. (2023). Single vs. multi-label: The issues, challenges and insights of contemporary classification schemes. Applied Sciences, 13(11): 6804. https://doi.org/10.3390/app13116804
[44] Gollapalli, M., Rahman, A., Alkharraa, M., Saraireh, L., AlKhulaifi, D., Salam, A.A., Krishnasamy, G., Alam Khan, M.A., Farooqui, M., Mahmud, M., Hatab, R. (2023). SUNFIT: A machine learning-based sustainable university field training framework for higher education. Sustainability, 15(10): 8057. https://doi.org/10.3390/su15108057
[45] Talha, M., Sarfraz, M., Rahman, A., Ghauri, S.A., Mohammad, R.M., Krishnasamy, G., Alkharraa, M. (2023). Voting-based deep convolutional neural networks (VB-DCNNs) for M-QAM and M-PSK signals classification. Electronics, 12(8): 1913. https://doi.org/10.3390/electronics12081913
[46] Basheer Ahmed, M.I., Alabdulkarem, H., Alomair, F. et al. (2023). A deep learning approach to driver drowsiness detection. Safety, 9(3): 65. https://doi.org/10.3390/safety9030065
[47] Musleh, D., Alotaibi, M., Alhaidari, F., Rahman, A., Mohammad, R.M. (2023). Intrusion Detection System Using Feature Extraction with Machine Learning Algorithms in IoT. Journal of Sensor and Actuator Networks, 12(2): 29. https://doi.org/10.3390/jsan12020029
[48] Qureshi, M.A., Asif, M., Anwar, S., Shaukat, U., Khan, M.A., Mosavi, A. (2023). Aspect level songs rating based upon reviews in English. Computers, Materials & Continua, 74(2): 2589-2605.
[49] Sajid, N.A., Ahmad, M., Rahman, A.U., Zaman, G., Ahmed, M.S., Ibrahim, N., Ahmed, M.I.B., Krishnasamy, G., Alzaher, R., Alkharraa, M., AlKhulaifi, D., AlQahtani, M., Salam, A.A., Saraireh, L., Gollapalli, M., Ahmed, R. (2023). A novel metadata based multi-label document classification technique. Computer Systems Science & Engineering, 46(2): 2195-2214. http://dx.doi.org/10.32604/csse.2023.033844
[50] Basheer Ahmed, M.I., Zaghdoud, R., Ahmed, M.S., Sendi, R., Alsharif, S., Alabdulkarim, J., Albin Saad, B.A., Alsabt, R., Rahman, A., Krishnasamy, G. (2023). A real-time computer vision based approach to detection and classification of traffic incidents. Big Data and Cognitive Computing, 7(1): 22. https://doi.org/10.3390/bdcc7010022
[51] Abbas, S., Raza, S.A., Khan, M.A., Khan, M.A., Sultan, K., Mosavi, A. (2023). Automated file labeling for heterogeneous files organization using machine learning. Computers, Materials & Continua, 74(2): 3263-3278.
[52] Basheer Ahmed, M.I., Saraireh, L., Rahman, A. et al. (2023). Personal protective equipment detection: A deep learning based sustainable approach. Sustainability, 15(18): 13990. https://doi.org/10.3390/su151813990
[53] ur Rahman, A. (2022). Geo-spatial disease clustering for public health decision making. Informatica, 46(6): 21-32. https://doi.org/10.31449/inf.v46i6.3827
[54] Khan, M.B.S., Nawaz, M.S., Ahmed, R., Khan, M.A., Mosavi, A. (2022). Intelligent breast cancer diagnostic system empowered by deep extreme gradient descent optimization. Mathematical Biosciences and Engineering, 19(8): 7978-8002. https://doi.org/10.3934/mbe.2022373
[55] Saqib, N.A., Salam, A.A., Atta-Ur-Rahman, Dash, S. (2021). Reviewing risks and vulnerabilities in web 2.0 for matching security considerations in web 3.0. Journal of Discrete Mathematical Sciences and Cryptography, 24(3): 809-825. https://doi.org/10.1080/09720529.2020.1857903